(NASA-TM-82363) EVALUATION OF A PNEUMATIC BOOT DEICING SYSTEM ON A GENERAL AVIATION WING MODEL (NASA) 35 p HC A03/MF A01
CSCL 01C

N81-25065

Unclas
G3/05 26542

THE UNIVERSITY OF KANSAS CENTER FOR RESEARCH, INC.
2291 Irving Hill Drive—Campus West
Lawrence, Kansas 66045

EVALUATION OF A PNEUMATIC BOOT DEICING SYSTEM ON A GENERAL AVIATION WING MODEL

KU-FRL-464-2

Prepared by

Alan E. Albright, David L. Kohlman, and William G. Schweikhard
University of Kansas
Lawrence, Kansas
and
Peggy Evanich
NASA Lewis Research Center
Cleveland, Ohio

for

Lewis Research Center
National Aeronautics and Space Administration
under NASA Grant NAG 3-71

Flight Research Laboratory
University of Kansas Center for Research, Inc.
Lawrence, Kansas 66045

June 1981

SUMMARY

A pneumatic boot deicing system was successfully tested on a Hicks modified 64 series airfoil wing model in the Icing Research Tunnel at NASA Lewis Research Center. Conclusions reached as a result of these tests are as follows:

1) Boot performance was not affected by tunnel total temperature or velocity.
2) Marginal effects in performance were associated with angle of attack.
3) Significant effects on performance were caused by variations in droplet size, LWC, ice cap thickness, inflation pressure, and surface treatment.

INTRODUCTION

The predominant ice protection system employed on light airplane wings and control surfaces today is a pneumatic boot system. This concept has been utilized since 1932 as a lightweight, simple, and practical way of removing ice. Recently, however, difficulty has been experienced in finding a boot configuration that will be effective on airfoils with large leading edge radii, a feature which characterizes several new low speed airfoils developed by NASA.

The purpose of these tests is twofold: first, to investigate the aerodynamic characteristics of a typical modern general aviation airfoil with and without a pneumatic boot ice protection system; and, second, to investigate the ice protection effectiveness of the boot. This includes 1) the change in drag on the airfoil with the boot inflated and deflated, 2) the change in drag due to primary and residual ice formation, 3) drag change due to cumulative residual ice formation, and 4) parameters affecting boot effectiveness.

During the July 1980 test period which is included in this report, tunnel and instrumentation difficulties were experienced. This caused the original test plan to be significantly abbreviated, as is obvious from the missing run numbers in Table 5. During July 1981 another week of testing is expected to take place using a modified boot on the same wing section tested in July 1980.

SYMBOLS

C_d	airfoil section drag coefficient
C_ℓ	airfoil section lift coefficient
$\bar{d}$	volume median-droplet diameter, μm
LWC	liquid water content, gm/m^3
p	boot inflation pressure, psig
t	icing spray time, min
T	total temperature, °F
V	free stream equivalent airspeed
V_l	local equivalent airspeed
WS	wing station
α	angle of attack, deg

TUNNEL DESCRIPTION

All the tests included in this report were performed in the Icing Research Tunnel (IRT) of the NASA Lewis Research Center, Cleveland, Ohio. The IRT is a closed cycle, atmospheric total pressure tunnel with a rectangular test section 1.83 m (6 ft) high by 2.74 m (9 ft) wide by 6.1 m (20 ft) long. Maximum tunnel airspeed with an empty test section is 134 m/sec (300 mph). A schematic of the

tunnel is shown in Figure 1.

A natural icing cloud is simulated by spraying water into the airstream upstream of the test section. This cloud is most uniform in the center of the test section covering a cross-sectional area of .9 m (3 ft) high by 1.5 m (5 ft) wide. The liquid water content can be varied from approximately 0.5 to over 2.4 gm/m^3 with volume-median droplet diameter range of 10 to 20 microns. Temperature is regulated by a 2100 ton cooler which can maintain the total temperature as low as -20°F.

MODEL DESCRIPTION

The wing section tested was taken from an actual single-engine light airplane. The original wing tapered from a NACA 64_2-A215 airfoil at the root (WS 0) to a NCAC 64_1-A412 airfoil at the tip (WS 216). The wing is twisted 0.167 degrees per foot of span (washout) with a chord taper of 1.1 inches per foot of span. The wing incorporated a modification proposed by Raymond Hicks (refs. 1, 2) of NASA Ames Research Center. This modification, which increases the thickness of the forward 32 percent of the upper surface, increases $C_{\ell_{max}}$, reduces C_d at high C_ℓ, and improves stall characteristics. This modification is seen in Figure 2 on a NACA 64_1-A412 airfoil.

The wing section tested was fastened securely to the turntable on the tunnel floor using the spar fittings that are used to attach the wing to the fuselage of the airplane. Figure 3 shows the wing section installed in the NASA IRT. The centerline of the tunnel lies at WS 58 of the original wing. Table 1 lists the airfoil coordinates of WS 58.

INSTRUMENTATION

A translating wake-survey probe was used to measure the section drag coefficient (C_d) of the test model. The probe, which consisted of a single stagnation pressure tube, was located about one chord length downstream of the airfoil at midspan. Drag wake surveys were taken only when the wind tunnel icing system was turned off. When the model was accreting ice, the survey probe was retracted behind a protective wind screen to prevent ice from being accumulated on the probe tip. As the probe translated laterally through the wake, a plot of the velocity decrement ratio (V_1/V) versus position was obtained. Integration of the wake defect gave a measurement of model section drag coefficient. Figure 4 is a schematic of the installation and instrumentation of the wake-survey.

The wing section was instrumented with 28 static pressure taps over both the upper and lower surface. Resulting local pressure coefficients were integrated to determine airfoil section lift and to determine the effect of ice accretion on pressure distribution. Approximately one-fourth of these taps were rendered ineffective when covered by the boot installation.

Accreted ice shapes were determined by one of two techniques depending on the amount of ice accreted. Both produced a paper tracing of the actual ice shape. Still photographs were taken of the wing model before and after pneumatic boot inflation. Movies at 24 frames per second were also taken during the inflation and shedding process.

DEICING SYSTEM DESCRIPTION

The deicing system tested consisted of a rubber pneumatic boot provided and manufactured by the B. F. Goodrich Company. The system was activated manually, causing the boot to inflate quickly. The intention is to break the bond of the ice on the flexing surface and allow the ice to be carried cleanly away by the airstream.

After all bare wing aerodynamic testing was completed, the boot was installed on the wing section in the center region of uniform ice accretion. The 25S type boot had a two-second inflation rate with a six-second total "on" time. Normally the boot was inflated with 18 psig. Three runs used 25 psig.

The boot's outside dimensions, as shown in Figure 5, are 12 inches in wrap-around width and 40 inches in the spanwise direction. The active region of the boot is 9 1/2 inches by 37 1/4 inches. The boot is constructed of nine spanwise tubes, four on the upper surface and five on the lower surface, as illustrated in Figure 6.

TEST CONDITIONS

For this series of tests, two test section equivalent airspeeds were chosen, 49.2 m/sec (96 knots) and 90.3 m/sec (175 knots). These speeds correspond approximately to the best rate of climb speed and the cruise speed of a high performance single-engine aircraft. The angle of attack values were defined as the local section angles of attack at the tunnel floor turntable.

Since the LWC and water droplet size ranges of the IRT icing cloud depended upon tunnel airspeed, operating envelopes for LWC and droplet size were plotted for the given airspeeds of interest, 49.2 m/sec and 90.3 m/sec (Figure

7). The LWC and droplet size were varied from .65 to 2.4 gm/m^3 and 11 to 20 microns, respectively. Figures 8 and 9 illustrate where the tunnel icing cloud test conditions are located on the continuous maximum and intermittent maximum icing condition curves specified in FAR Part 25 (ref. 3).

The type of ice (i.e., glaze or rime) that formed on the airfoil depended primarily on the tunnel total air temperature. To produce glaze ice, the tunnel total air temperature was set at -3.9°C (25°F); to produce rime ice, it was set at -15°C (5°F). The ambient or outside air temperature (OAT) corresponds to the static air temperature in the tunnel test section. For the two airspeeds chosen, namely 49.2 m/sec and 90.3 m/sec, the OAT's for glaze ice were -5.1°C and -7.8°C, respectively; and the OAT's for rime ice were -16.2°C and -18°C, respectively. The true airspeeds were 43.7 m/sec and 85.3 m/sec at T = 5°F and 44.7 m/sec and 86.9 m/sec at T = 25°F.

Time of icing (water spray) was dependent on LWC, droplet size, and ice thickness desired. Ice [illegible]ses, measured normal to the leading edge at each angle of attack with a telescope and calibrated scale, ranged from 1/4 inch to 1 1/4 inches by varying the icing spray time from 5 minutes to 12 minutes. Three test runs were conducted with approximately 20 minutes of continuous spray. Table 2 is a summary of the range of test conditions chosen.

Ice type (rime or glaze) is a function of LWC as well as temperature. Although the two temperatures of 5°F and 25°F were chosen to produce either rime ice or glaze ice, pure rime or glaze ice was occasionally not achieved, as the LWC was varied at each temperature setting. Fluctuations of plus or minus 2°F were common during the runs.

TEST RESULTS

Aerodynamic Penalties from Boot Installation and Inflation

A pneumatic boot installed on a wing will affect aircraft performance even when the aircraft is not flying in icing conditions. Since the drag changes are small, the results are especially sensitive to the inaccuracy of the drag wake survey. Figures 10 and 11 show the drag of the wing section with a pneumatic boot, inflated and deflated, compared to that of the bare wing. At 96 knots, over the range of angles of attack from -2° to 10°, installing the boot increased drag an average of 8%. At 175 knots, the results show that installing the boot had a negligible effect on drag. Table 3 is a list of the airfoil drag coefficients with the boot installed.

Effect of Ice Accretion on Drag and Lift with Boot Inoperative

Typical rime ice formations are characteristic of low air temperatures and low icing rates. The accreted ice shape is relatively streamlined, as shown in Figure 12 with minimal aerodynamic penalties. A continuous 15 minute ice spray at 5°F, LWC = .80, increased drag by 123% compared to the clean wing with boot deflated. Figures 13 and 14 show the effect of ice accretion on drag at 96 and 175 knots.

At higher temperatures and icing rates, a rougher and more irregular shape of glaze ice accumulates. Typically, two distinct ridges are formed, as shown in Figure 15, one on the upper surface and one on the lower surface. Glaze ice causes significant aerodynamic penalties, more so than rime ice. After a 15 minute ice spray with T = 25°F, LWC = .80, the airfoil drag increased 411%.

An ice accretion formed at a low to moderate angle of attack can greatly increase drag when the angle of attack is increased during a normal landing approach. Glaze ice was allowed to accumulate on the model for 10 minutes with LWC = 2.4 gm/m^3 and α = 7.8°. After measurements were taken to determine lift and drag, the angle of attack was increased to 10°, where measurements were again taken. Drag was integrated from the wake-survey, and lift was integrated from the static pressure profile of the airfoil. At the original α of 7.8°, the ice formation increased drag 322% and decreased lift 18%. With the same ice shape, drag increased to 665% over that of the clean wing at α = 10°, with a 23% decrease in lift.

Airfoil Characteristics with Boot Operating

Photographs showing deicing performance of the untreated spanwise-tube pneumatic boot are shown in Figure 16 as a total shed, and in Figure 17 as a partial shed. The untreated boot inflations generally resulted in a significant amount of residual ice on the boot. Consequently, airfoil drag after boot inflation is normally greater than the clean airfoil drag. This drag increase resulting from residual ice on the airfoil after the boot is activated is a direct measure of the deicer effectiveness.

Since the drag wake-survey provided results for only a limited number of runs, the total ice shed of the center 52 cm section of the boot, as listed in the last column of Table 5, is also used as a direct measure of the deicer effectiveness. These values were agreed upon by two persons conducting the research and checked later by a third person from pictures taken during the testing.

Air total temperature apparently has negligible effect on ice removal, as the average total ice shed at 25°F (glaze ice) was 49%, while at 5°F (rime ice) the ice shed increased to only 50%. For a given liquid water content and droplet size, the deicer effectiveness was also not affected by tunnel airspeed. At 175 knots the average total ice shed was 44%, while at 96 knots the ice shed increased to 45% at a LWC of 1.16 gm/m^3 and with a constant volume-median droplet diameter size of 15 μm.

Boot effectiveness was marginally affected by the angle of attack at which the ice shape was formed and shed. At an angle of attack of 1.2°, the average total ice shed was 43%, while at α = 7.8° it reduced to 36%.

Liquid water content was found to have an effect on boot performance, as illustrated in Figure 18. A comparison using runs with spray times between 5 and 8 minutes, constant velocity, and constant droplet size show that the average total ice shed with a LWC of 1.16 gm/m^3 is 45%. An increase in LWC to 1.50 gm/m^3 decreased the average ice shed to 32%.

A similar comparison was made with runs of LWC = 1.50 gm/m^3 and $\bar{d}$ = 15 μm against runs of LWC = 2.40 gm/m^3 and $\bar{d}$ = 20 μm. With the LWC of 1.50 gm/m^3, the average total ice shed was again 32%; but with the higher LWC and droplet size the ice shed decreased to 23%. This difference may be a result of increased surface extent of residual ice due to impingement farther aft with the increased droplet size.

Deicer effectiveness was greatly affected by icing time (ice thickness) before initial inflation of the boot, as shown in Figure 18. With a LWC of 1.16 gm/m^3, the total ice shed ranged from 36% after a 5 minute spray to 80% after a 12 minute spray. At a higher LWC of 1.50 gm/m^3, the percentage ranged from 10% to 95%. This clearly demonstrates that premature inflation of a boot

before a significant ice cap has accumulated may actually reduce the chance of removing the ice.

Effect of Various Modes of Boot Operation on Ice Removal

Three runs were conducted with an increased boot inflation pressure of 25 psig, instead of the normal 18 psig. Comparing two of these runs with two identical runs, except for inflation pressure, shows that with 18 psig the total ice sheds were 20% and 40%, while increasing the inflation pressure to 25 psig increased the percentages to 77% and 80%. However, it is felt that more runs are necessary for comparison before generalizing that a higher inflation pressure will always produce such a significant improvement in boot effectiveness.

Three other runs were conducted to simulate an airplane flying through a continuous icing cloud during which the pilot activates the boot after a small amount of ice has accumulated, and then repeates activation every 1 1/2 minutes in a cyclic fashion. The total icing time for these runs was in excess of 20 minutes. The deicer boot was effective in handling this type of inflation sequence with a 75% to 100% shed generally occurring every 3 minutes (every other inflation), while not allowing the ice cap to grow much beyond 1/2 inch thick

Specific regions of the boot surface were treated with two chemical coatings designed to reduce ice adhesion. ICEX, a silicon-based fluid coating, provided by B. F. Goodrich, was applied to the boot in the locations described in Table 4 and for the runs as noted in Table 5. The original test plan included more extensive tests with ICEX, but due to tunnel breakdowns these runs were eliminated. The deicer effectiveness improved greatly with ICEX, as shown

in Figures 19 and 20. All six runs with ICEX resulted in 90% to 100% shedding of the total ice cap.

The second chemical was tested on a trial basis and is not designed for normal use on a pneumatic boot. The chemical, a silicone grease manufactured by the GE Silicone Products Division, Waterford, New York, was applied to the lower 25 cm of the boot, as shown in Figure 3. As illustrated in Figures 21 and 22, this icephobic also greatly improved the boot effectiveness. However, the effective lift span of the icephobic was found to be approximately six runs.

CONCLUSIONS

The effectiveness of the pneumatic boot system was determined by the percentage increase in airfoil drag after inflation over the clean wing, and by the percentage of the total ice cap shed. Conclusions reached as a result of these tests are as follows:

1. With the deicer inoperative, a 15 minute rime ice accumulation increased airfoil drag 123%, while a 15 minute glaze ice accumulation increased airfoil drag 411%.
2. An ice shape formed at $\alpha = 7.8°$ increased drag 322%, while increasing α to 10° with the same ice shape increased drag 665% over that of the clean wing at $\alpha = 10°$.
3. Air total temperature and velocity have negligible effect on boot performance over the ranges tested.
4. Boot performance was marginally affected by the angle of attack. At $\alpha = 1.2°$, the average total ice shed was 43%, while at $\alpha = 7.8°$ it

reduced to 36% for the untreated boot.

5. An increase in LWC from 1.16 gm/m^3 to 1.50 gm/m^3 with constant droplet size and ice spray times decreased the average total ice shed from 45% to 32%. A further increase in LWC to 2.40 gm/m^3 with an increase in dorplet size reduced the average total ice shed to 23%.
6. Boot performance is greatly affected by the length of time of ice buildup (ice thickness) before initial boot inflation. With a LWC of 1.50 gm/m^3, after a 5 minute spray only 10% of the ice was shed, while after a 12 minute spray the ice shed increased to 95% of the total ice cap. Similar results were found at a LWC of 1.16 gm/m^3.
7. Increasing the boot inflation pressure from 18 psig to 25 psig increased the deicer effectiveness.
8. The boot was satisfactory in removing ice during a 20 minute continuous ice spray during which the boot was activated every 1 1/2 minutes.
9. Boot surface coatings caused significant improvements in ice removal effectiveness. ICEX increased the average total ice shed to over 90%. An icephobic paste had a similar effect but with a much shorter life span than ICEX.

The scope of this investigation of the pneumatic boot system was limited due to tunnel and instrumentation breakdowns. Therefore, the actual performance of the boot should not be extrapolated beyond the results of this report.

REFERENCES

1. Hicks, R. M., and Schairer, E. T., "Effects of Upper Surface Modifications on the Aerodynamic Characteristics of the NACA 63_2-215 Airfoil Section." NASA TM 78503, January 1979.

2. Szelazek, C. A., and Hicks, R. M., "Upper-Surface Modifications for $C_{\ell_{max}}$ Improvement of Selected NACA 6-Series Airfoils." NASA TM 78603, August 1979.

3. Federal Aviation Regulations, Part 25, Appendix C - Airworthiness Standards: Transport Category Airplanes. Department of Transportation, Federal Aviation Adminstration, Washington, D.C., June 1974.

Table 1: Airfoil Coordinates of Wing Section at Centerline of the IRT (WS 58) in percent of chord.

Upper Surface		Lower Surface	
x	y	x	y
0	-.704	0	-.704
.015	-.250	.335	-1.474
.648	.791	.723	-1.858
1.138	2.372	1.216	-2.193
2.055	3.447	2.451	-2.760
3.953	4.941	4.926	-3.545
6.324	6.008	7.407	-4.130
9.486	6.735	14.223	-5.371
11.352	7.036	19.197	-5.395
13.439	7.502	24.175	-6.359
22.024	7.565	29.157	-6.658
24.996	7.581	34.142	-6.816
30.126	7.597	39.129	-6.870
34.783	7.534	44.122	-6.718
39.428	7.426	49.115	-6.449
44.409	7.110	54.111	-6.114
49.387	6.591	99.741	-2.794
54.360	5.891		
59.331	5.047		
62.111	4.526		
99.744	-2.606		

Table 2: Range of Test Conditions

Equivalent airspeed, knots	96 and 175
Angle of attack, deg	1.2, 4.5, and 7.8
Total temperature, ^{o}F	5 and 25
Liquid water content, gm/m^3	.80 to 2.40
Volume-median droplet diameter, microns	11 to 20
Icing time, minutes	1.0 to 20

Table 3: Aerodynamic Data with Boot Installed

RUN #	α deg	V Knots	C_d
	BOOT DEFLATED		
1A	-2.0	96	.0116
2A	- .5	96	.0108
3A	1.2	96	.0112
4A	7.8	96	.0119
6A	-2.0	175	.0119
7A	- .5	175	.0110
8A	1.2	175	.0105
9A	7.8	175	.0113
10A	10.0	175	.0120
	BOOT INFLATED		
11A	-2.0	96	.0162
12A	- .5	96	.0151
13A	1.2	96	.0146
14A	7.8	96	.0168
16A	-2.0	175	.0162
17A	- .5	175	.0145
18A	1.2	175	.0136
19A	7.8	175	.0183
20A	10.0	175	.0199

Table 4: Boot Treatment Description

Code	Region	Treatment
o	entire boot	Untreated
Δ	top 25 cm:	ICEX
	middle 52 cm:	Untreated
	bottom 25 cm:	Icephobic grease
□	top 77 cm:	ICEX
	bottom 25 cm:	Icephobic grease

Table 5: Boot Performance Summary

CODE	RUN #	α deg	V Knots	LWC $_3$ gm/m	$\bar{d}$ μm	T_F	t min	p psig	C_d before inflation	C_d after inflation	ice thickness inch	TOTAL PERCENTAGE SHED 0 25 50 75 100
O	1	1.2	96	1.16	15	25	5	18		.0105	1/4	
O	2	1.2	96	1.16	15	25	8	18	.0123	.0106	5/8	
O	3	1.2	96	1.16	15	25	12	18			7/8	
O	4	1.2	96	1.50	15	25	5	18		.0144	1/4	
O	5	1.2	96	1.50	15	25	8	18			3/4	
O	05	1.2	96	1.50	15	25+	8	18	.0157	.0129	3/4	
O	6	1.2	96	1.50	15	25	12	18		.0167	1	
O	8	7.8	96	2.40	20	25+	8	18	.0220	.0166	5/8	not recorded
O	10	7.8	96	1.16	15	25	5	18		.0134	1/4	
O	12	7.8	96	1.16	15	25	12	18		.0159	3/4	
O	13	7.8	96	1.50	15	25	5	18		.0162	1/4	
O	15	7.8	96	1.50	15	25	12	18		.0170	1	
▲	20	7.8	96	2.40	20	5	6	18			1/2	
▲	21	4.5	96	2.40	20	5	6	18			1/2	
▲	22	1.2	96	2.40	20	5	6	18			5/8	
▲	23	7.8	175	1.16	15	5	6	18			5/8	
▲	24	4.5	175	1.16	15	5	6	18		.0153	5/8	
▲	27	7.8	96	2.40	20	5	6	25		.0198	1/2	
▲	33	7.8	96	2.40	20	5	20	18				
▲	40	7.8	96	2.40	20	25	8	18	.0247	.0187	5/8	
▲	41	[illegible]	96	2.40	20	25	6	18	.0222		1/2	
▲	42	1.2	96	2.40	20	25	6	18		.0157	1/4	
▲	43	7.8	175	1.16	15	25	8	18		.0189	1 1/4	
▲	44	4.5	175	1.16	15	25	6	18		.0147	3/4	
▲	45	1.2	175	1.16	15	25	6	18	.0203	.0185	1/2	
▲	46	1.2	175	1.16	15	25	6	25		.0130	1/2	
▲	47	7.8	96	2.40	20	25	8	25			5/8	
▲	53	7.8	96	2.40	20	25	20	18				
□	60	7.8	96	2.40	20	25	8	18			1/2	
□	62	1.2	96	2.40	20	5	6	18			1/2	
□	63	1.2	175	1.16	15	5+	6	18			3/4	
□	65	1.2	175	1.16	15	25	6	18			1/2	
□	73	7.8	96	2.40	20	5	20	18				
□	80	7.8	96	2.40	20	5	8	18			3/4	

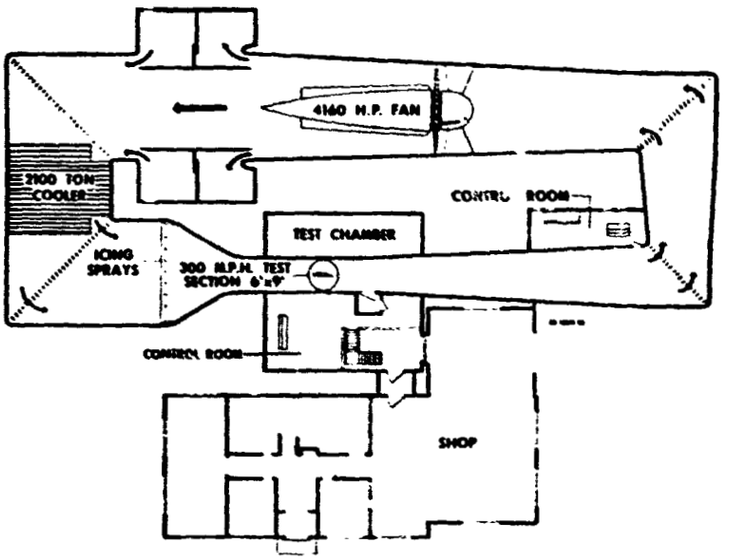

Figure 1. - NASA Lewis Icing Research Tunnel.

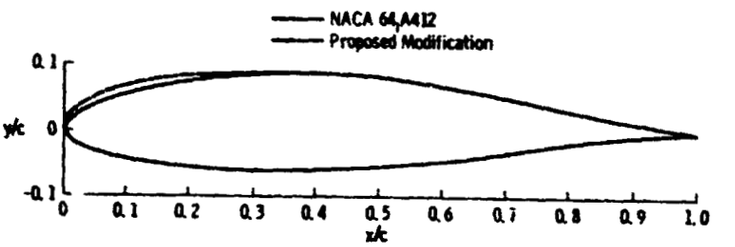

Figure 2. - Hicks Modification on a NACA 64_1-A412 Airfoil.

Figure 3. - Application of Icephobic on Wing Section Installed in the NASA Lewis Icing Research Tunnel.

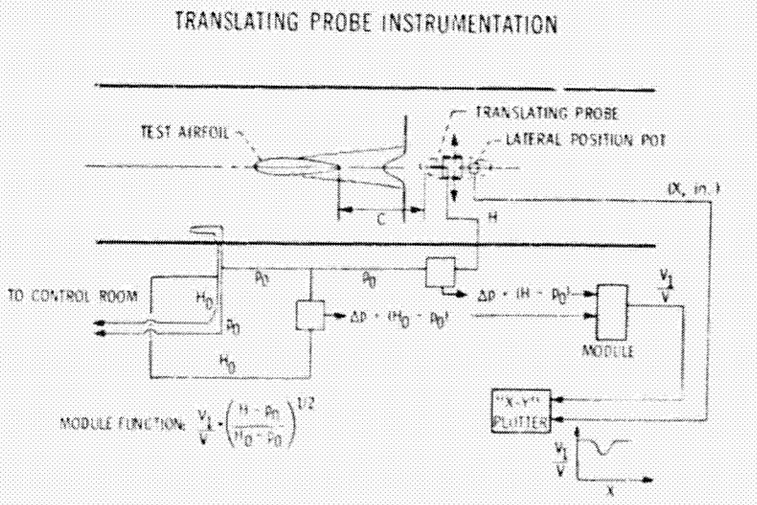

Figure 4. - Schematic of Wake-Survey Probe Instrumentation.

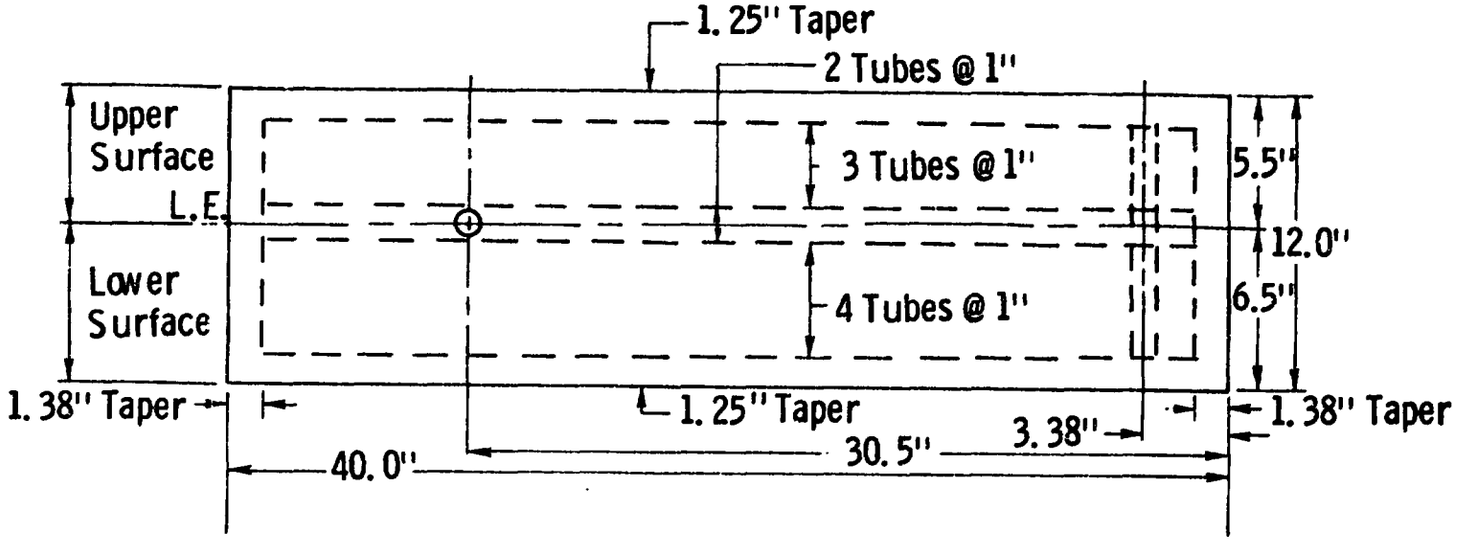

Figure 5. - Layout of Type 25S Pneumatic Boot Tested on a 642-A215 Hicks Modified Airfoil in the Icing Research Tunnel.

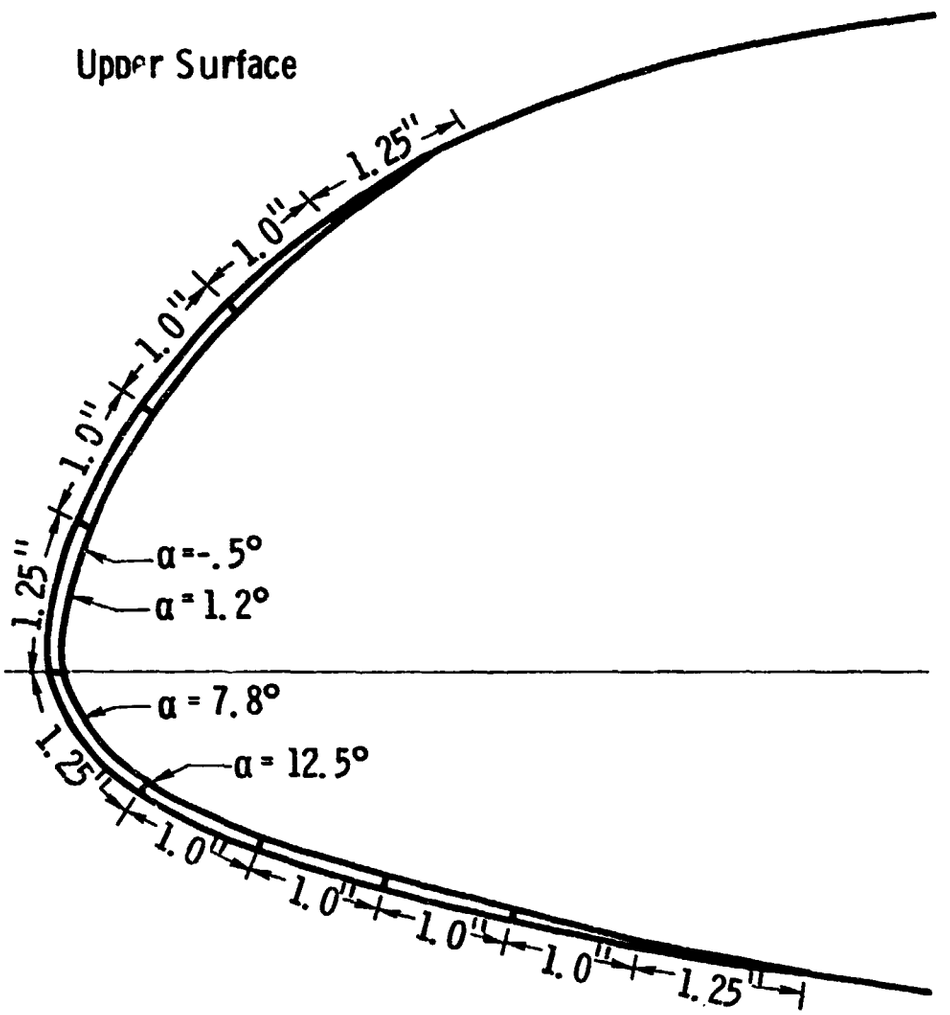

Figure 6. - Pneumatic Boot Installed on Wing at WS 58 with Angles of Attack Locations.

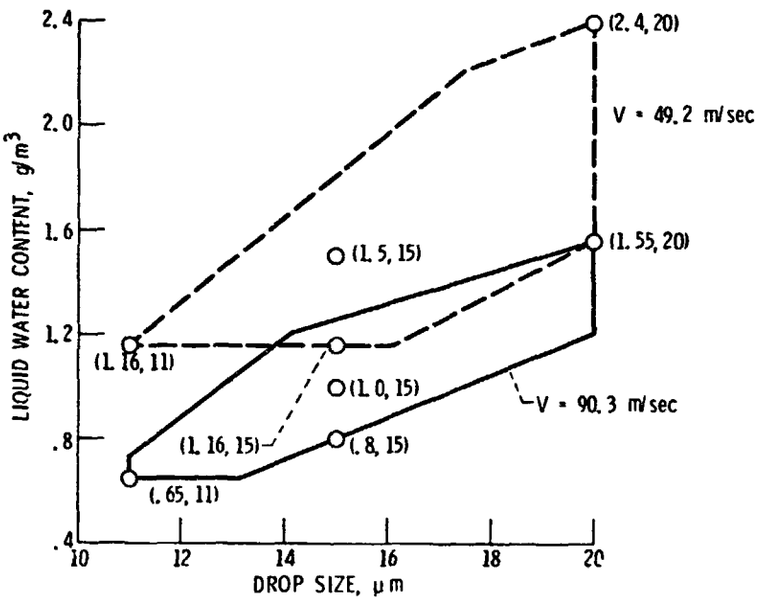

Figure 7. - IRT Operating Envelopes and Test Points.

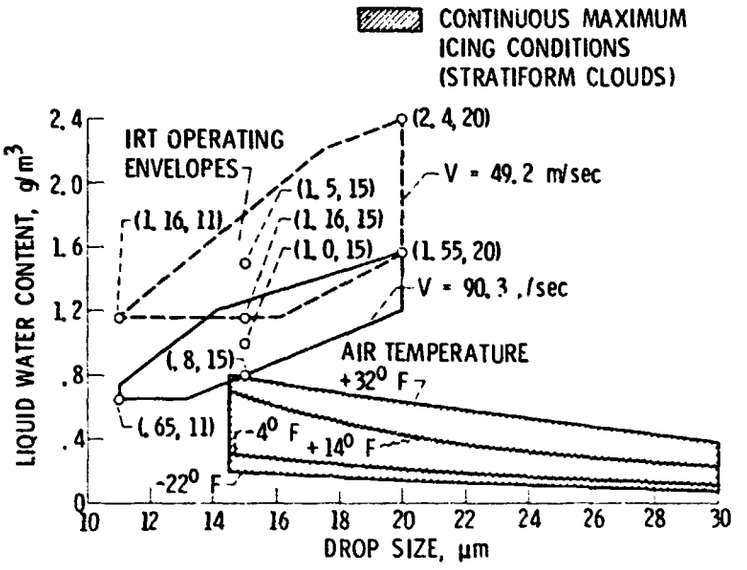

Figure 8. - Continuous Maximum Icing Conditions (ref. 3) and IRT Operating Envelopes.

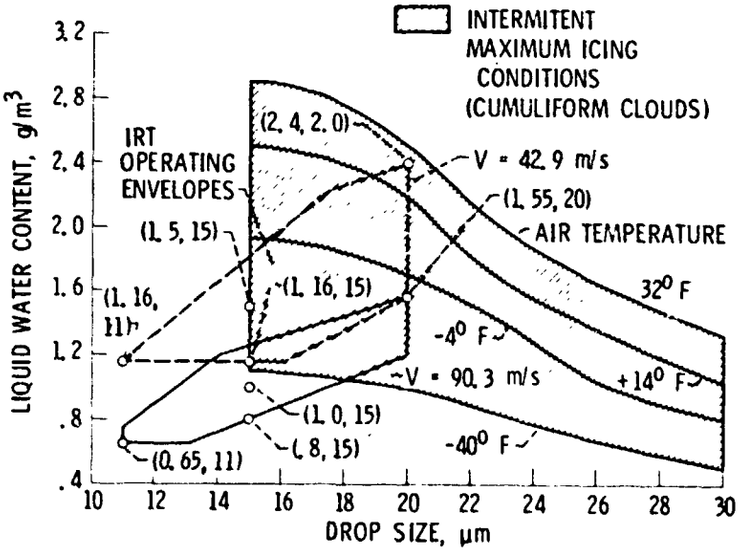

Figure 9. - Intermittent Maximum Icing Conditions (ref. 3) and Operating Envelopes.

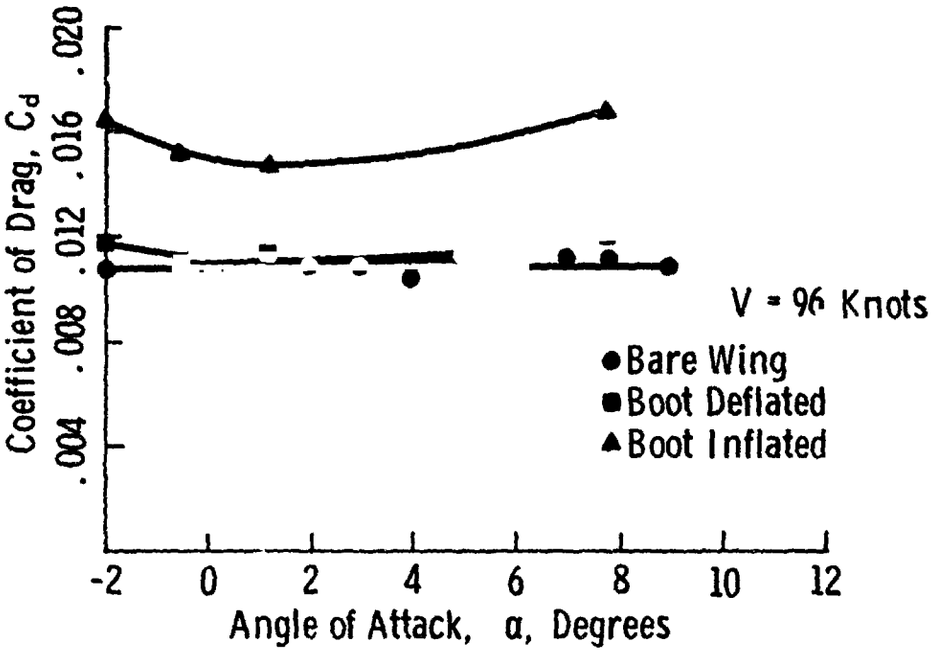

Figure 10. Drag Penalty from Boot Installation at 96 knots.

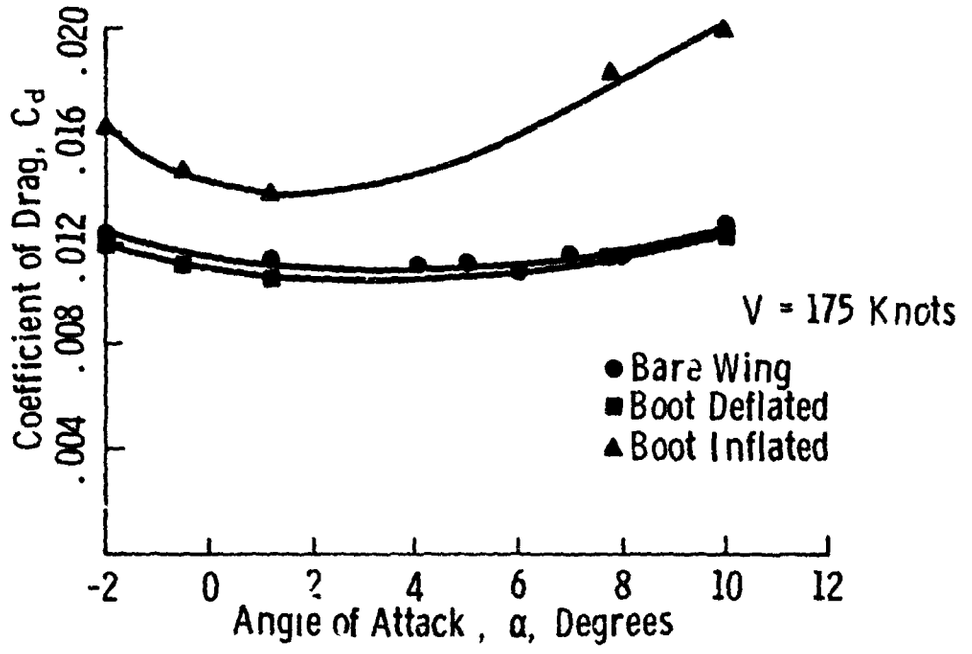

Figure 11. - Drag Penalty from Boot Installation at 175 Knots.

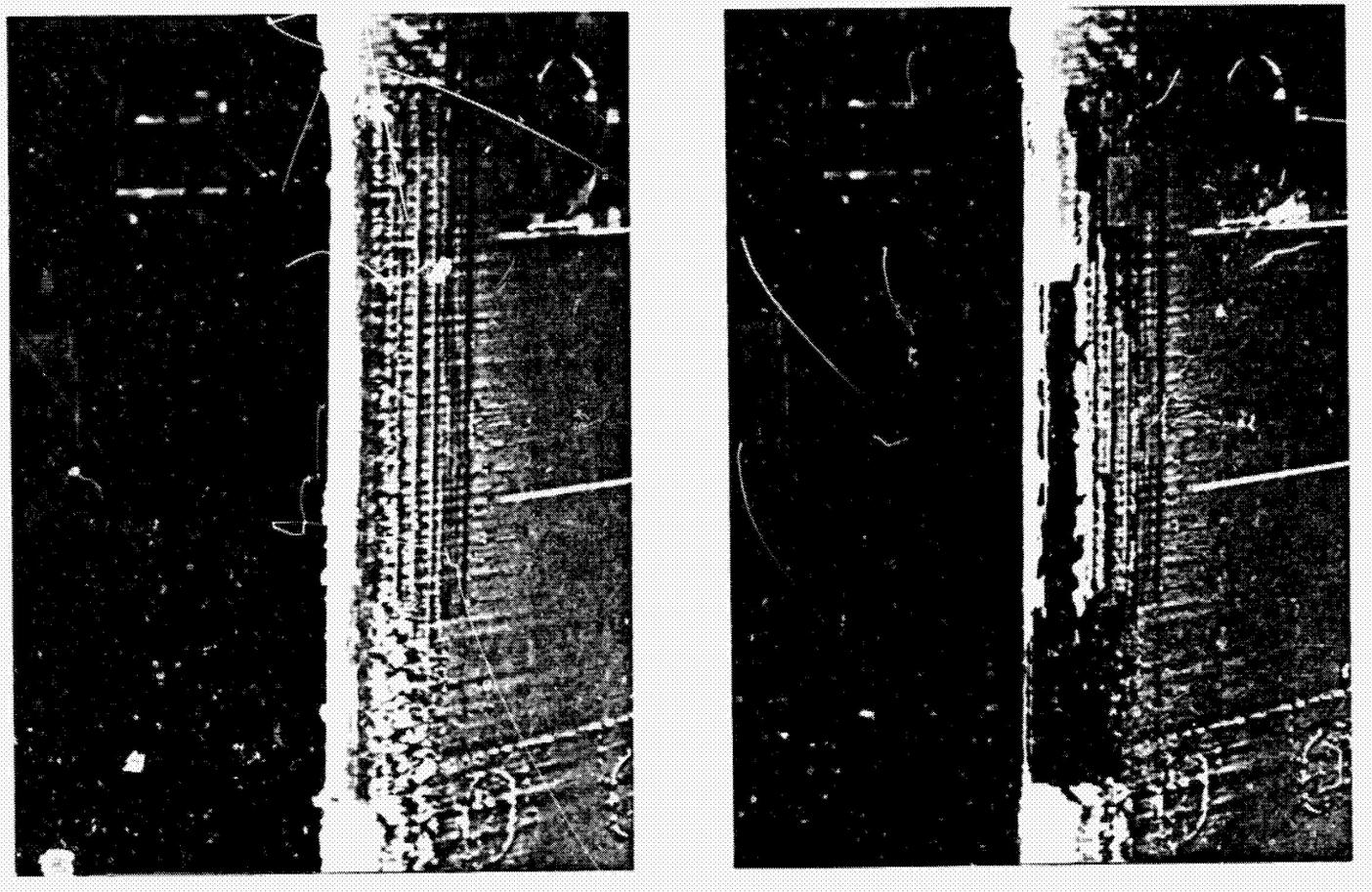

(a) Before Inflation

(b) After Inflation

Figure 12. - Run 27; α = 7.8°, V = 96 ", LWC = 2.40 gm/m^3, μm, T = 5°F, t = 6 min.

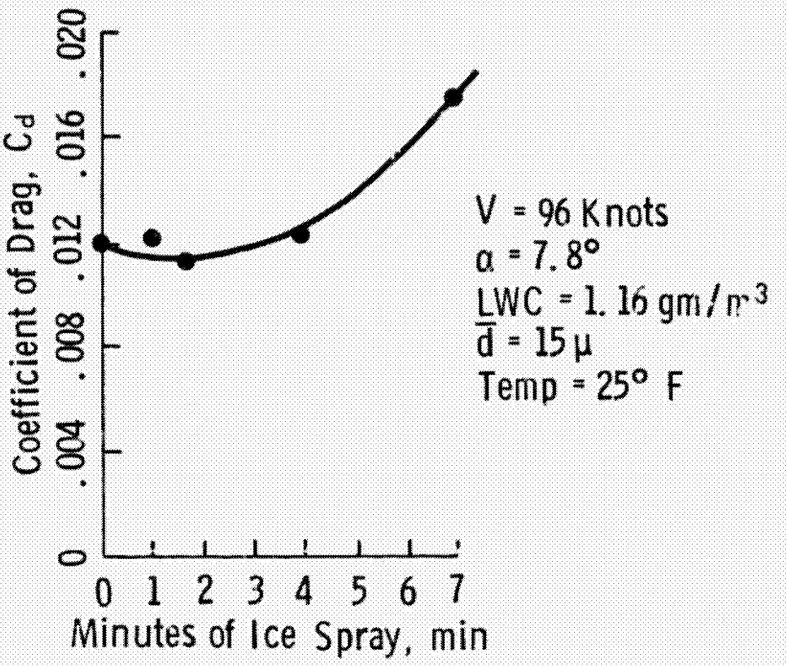

Figure 13. - Drag Penalty from Ice Buildup at 96 Knots.

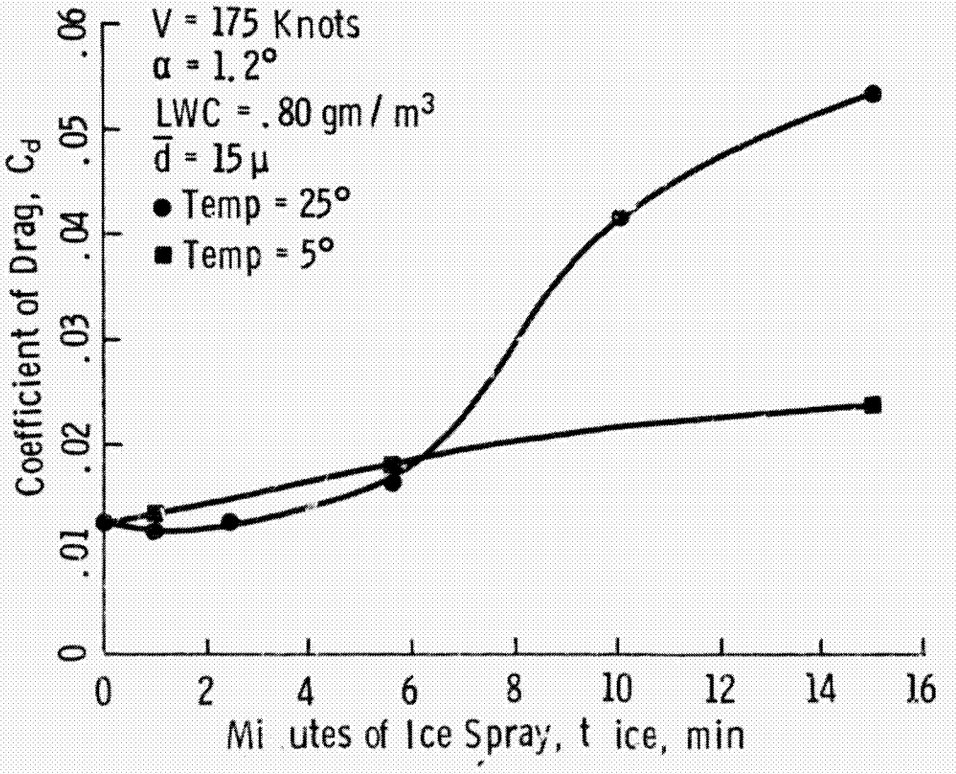

Figure 14. - Drag Penalty from Ice Buildup at 175 Knots.

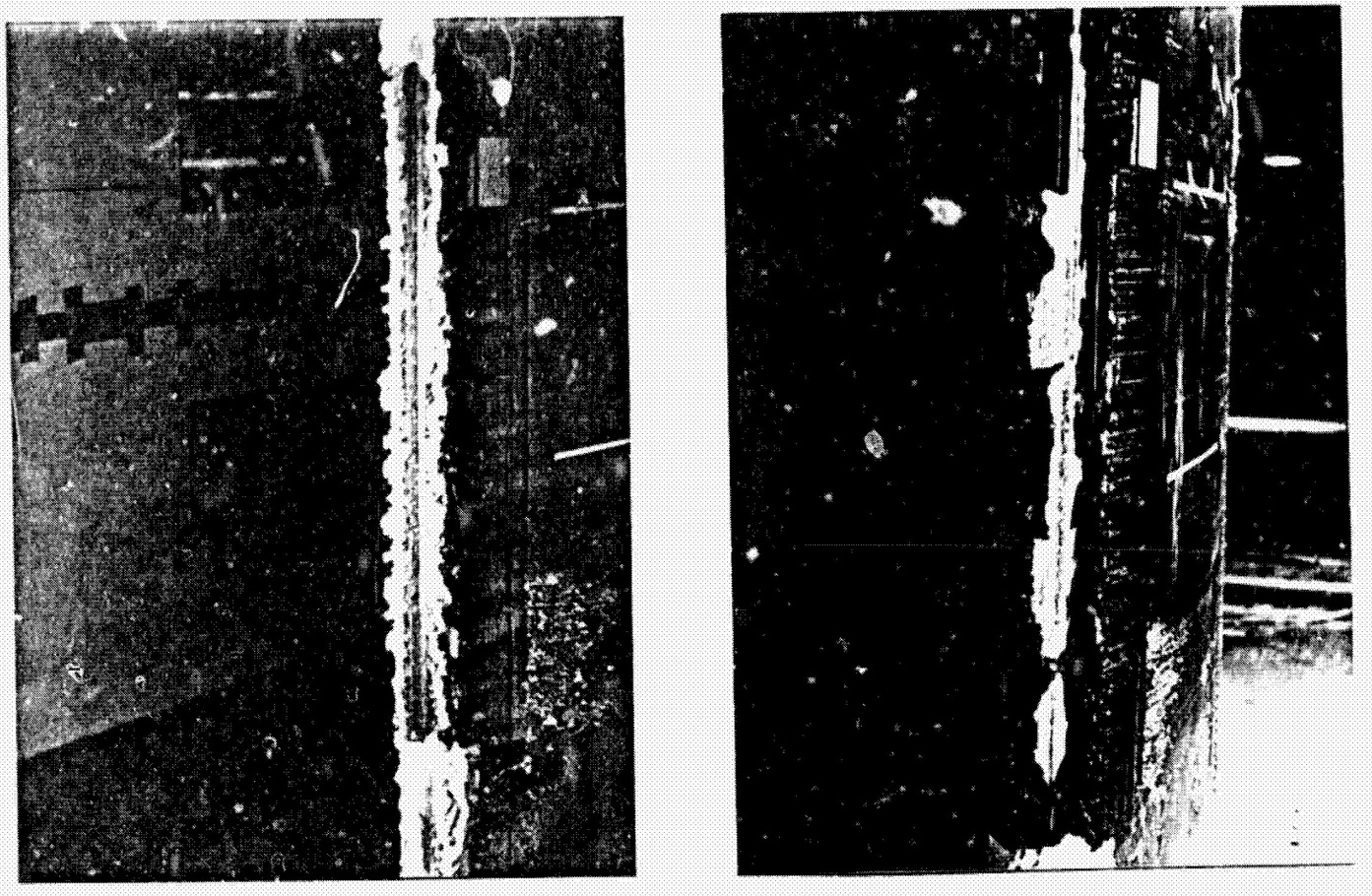

(a) Before Inflation

(b) After Inflation

Figure 15. - Run 45; α = 1.2°, V = 175 K, LWC = 1.16 gm/m^3, $\bar{d}$ = 15 μm, T = 25°F, t = 6 min.

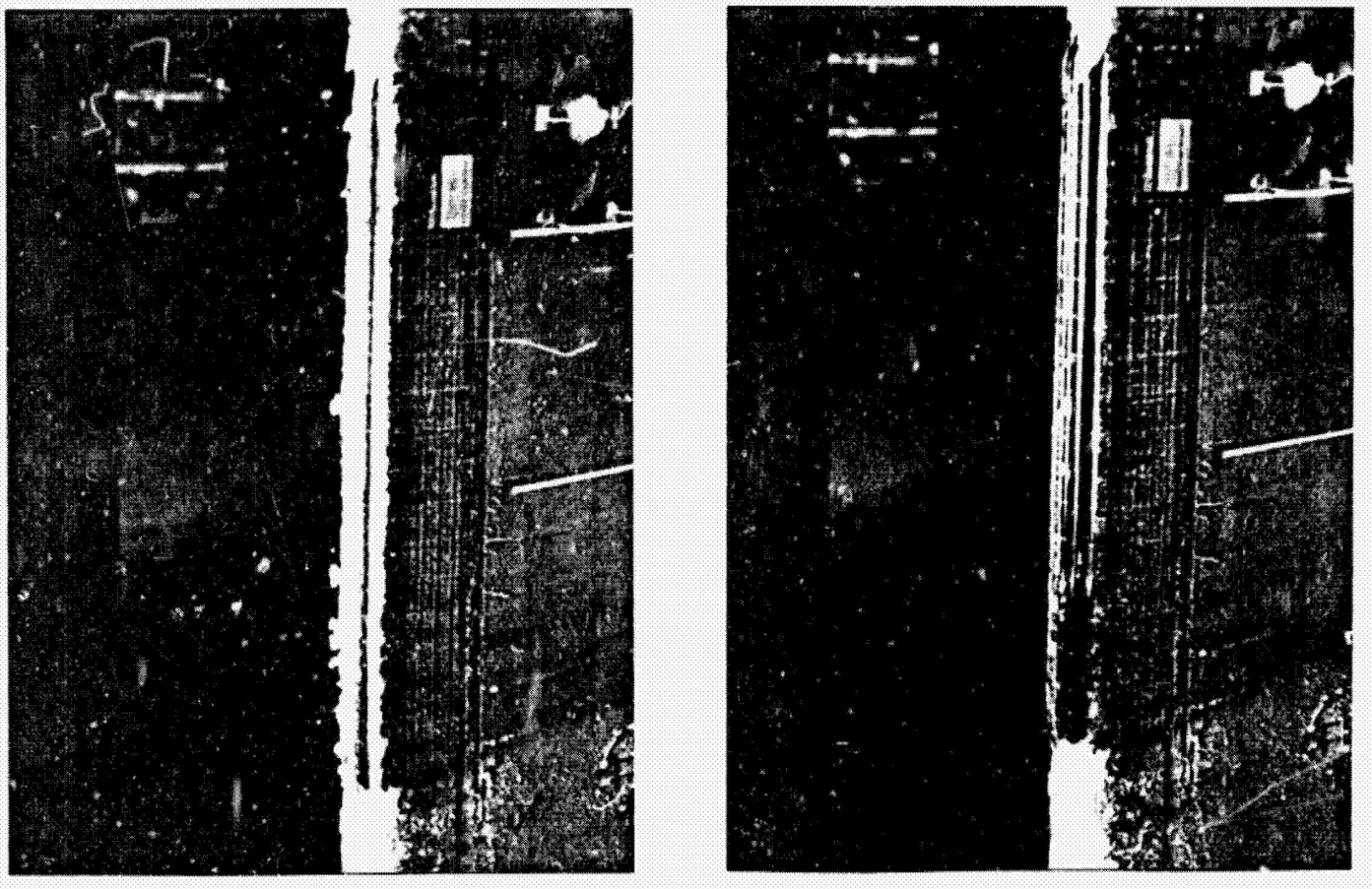

(a) Before Inflation

(b) After Inflation

Figure 16. - Run 6; α = 1.2°, V = 96 K, LWC = 1.50 gm/m^3, $\bar{d}$ = 15 μm, T = 25°F, t = 12 min.

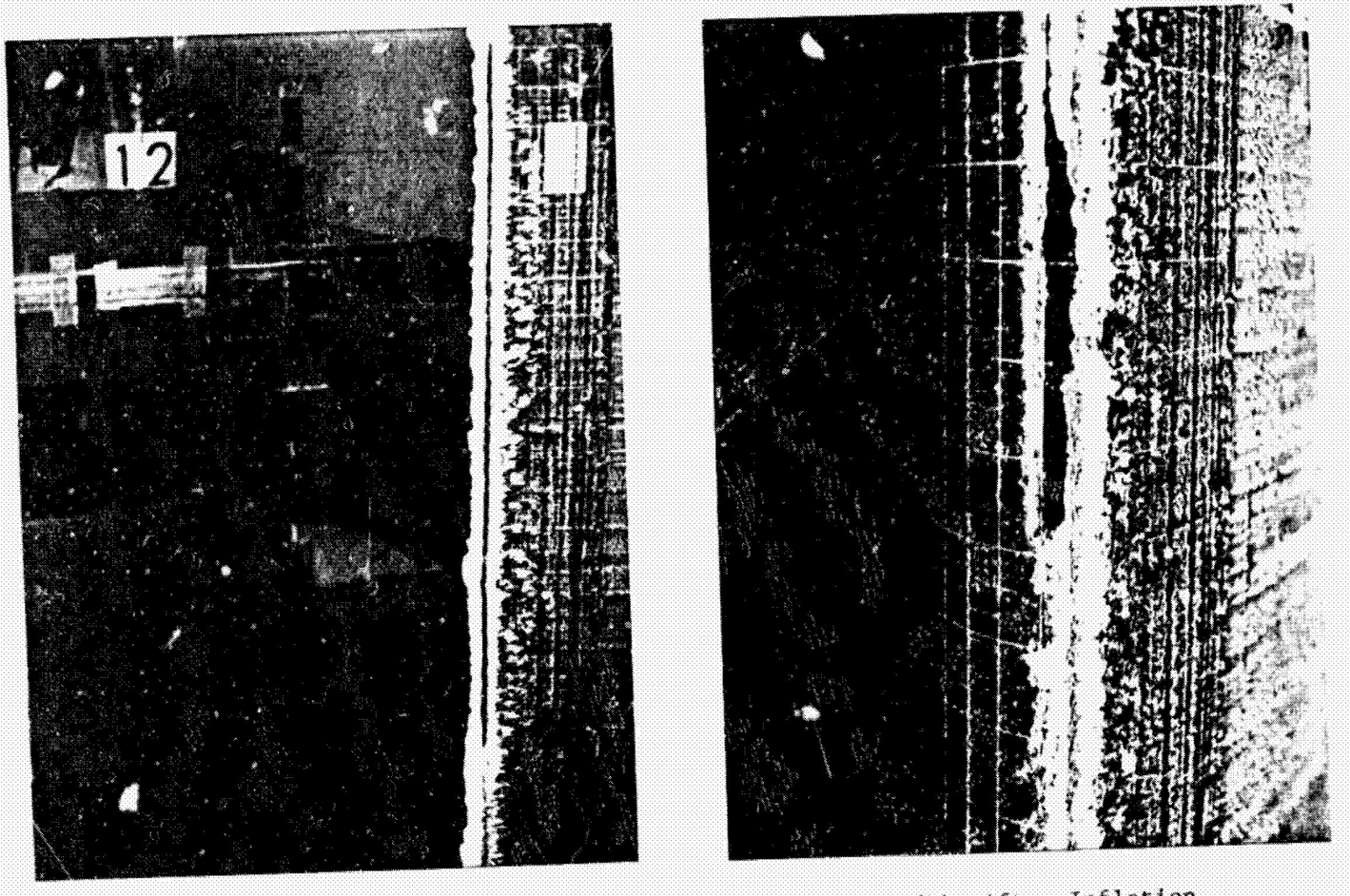

(a) Before Inflation

(b) After Inflation

Figure 17. - Run 12; α = 1.2°, V = 96 K, LWC = 2.40 gm/m^3, $\bar{d}$ = 20 μm, T = 5°F, t = 6 min.

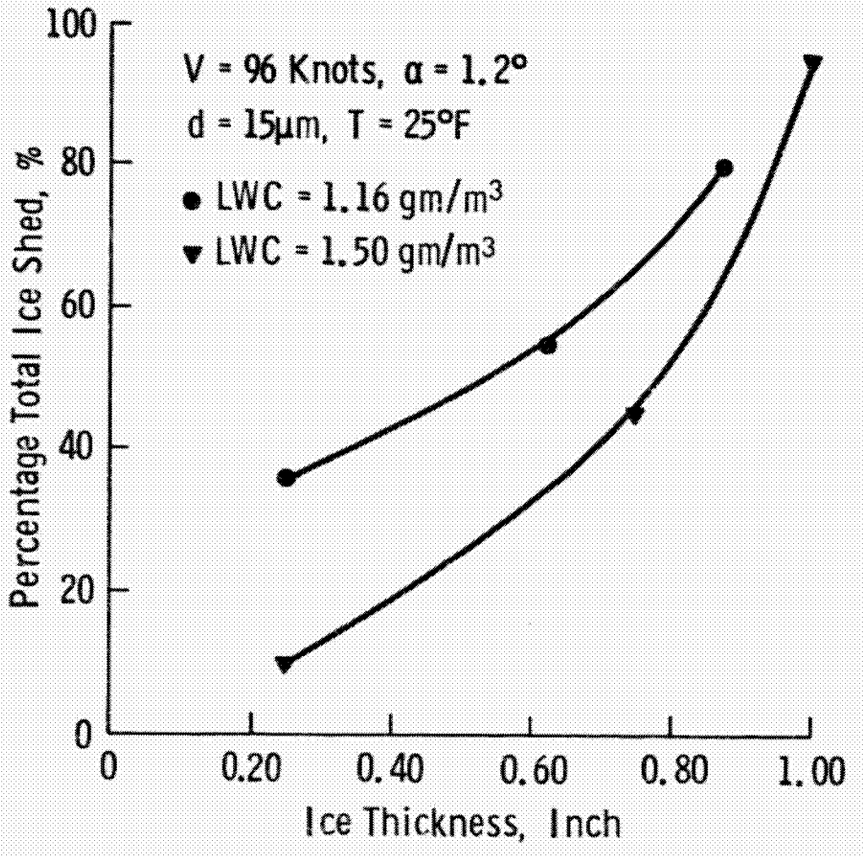

Figure 18. - Effect of Ice Cap Thickness on Total Ice Shed.

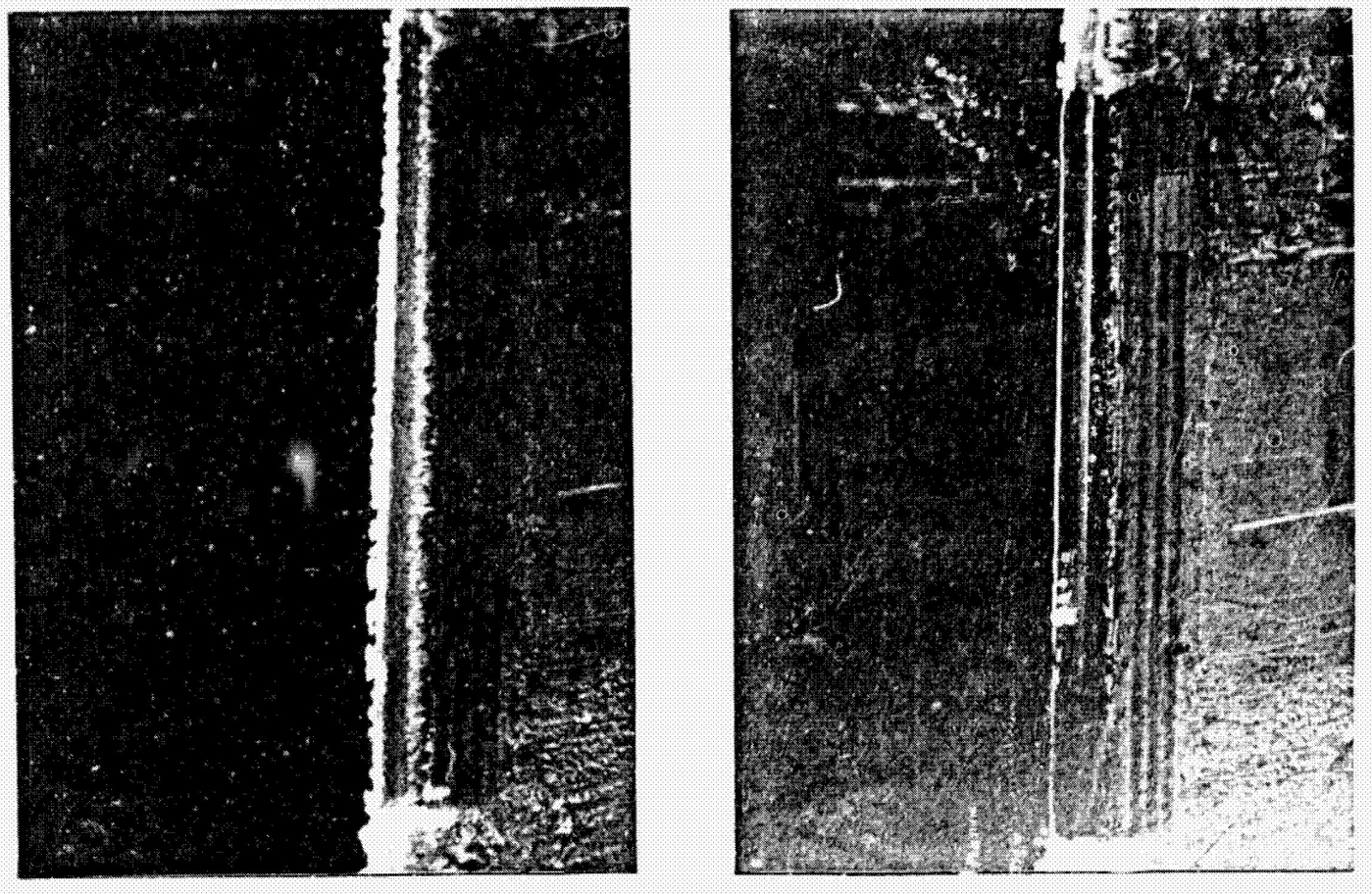

(a) Before Inflation

(b) After Inflation

Figure 19. - Run 62; with ICEX, α = 1.2°, V = 96 K, LWC = 2.40 gm/m^3, $\bar{d}$ = 20 μm, T = 5°F, t = 6 min.

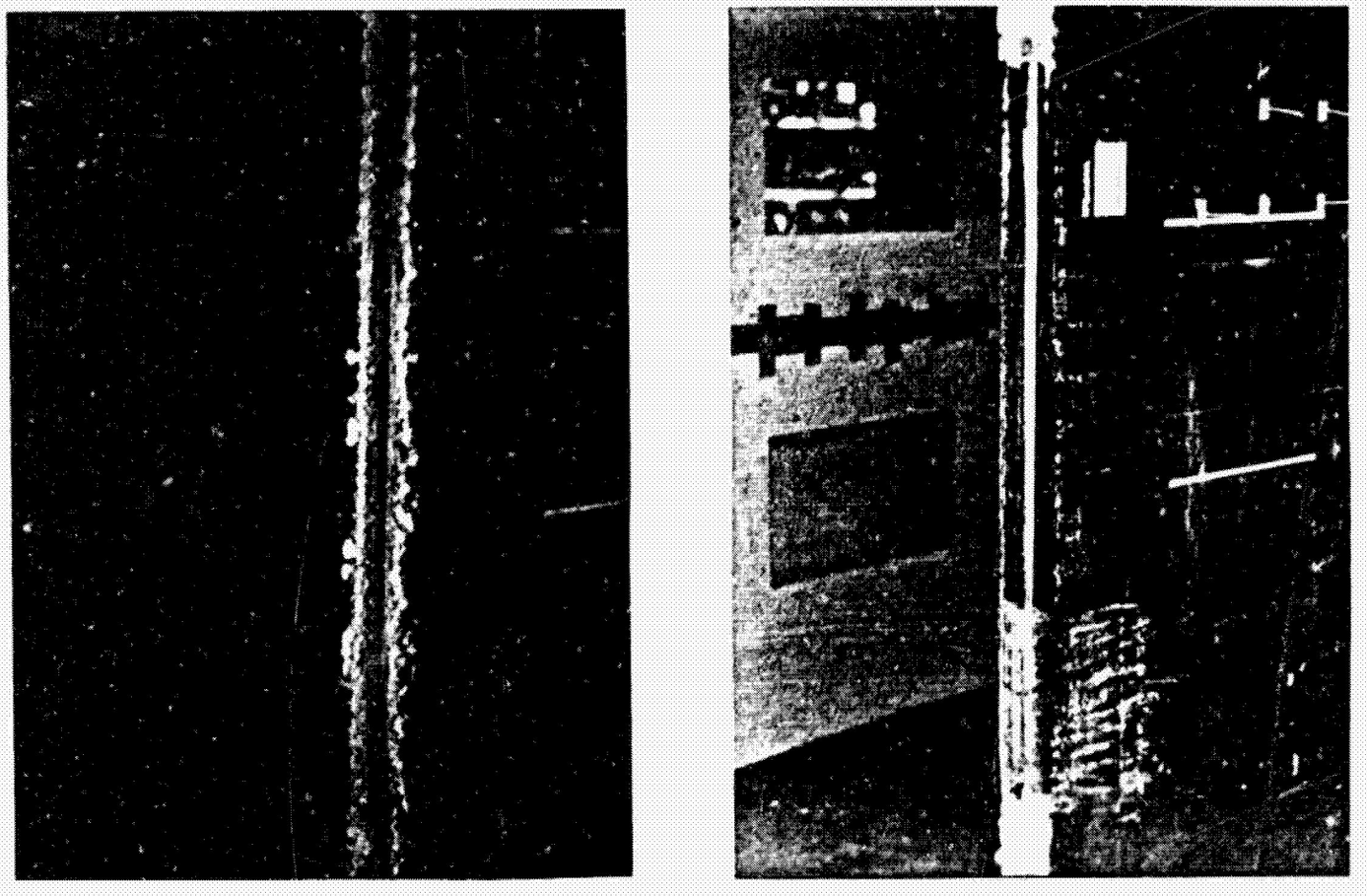

(a) Before Inflation

(b) After Inflation

Figure 20. - Run 65; with ICEX, α = 1.2°, V = 175 K, LWC = 1.16 gm/m^3, $\bar{d}$ = 15 μm, T = 25°F, t = 6 min.

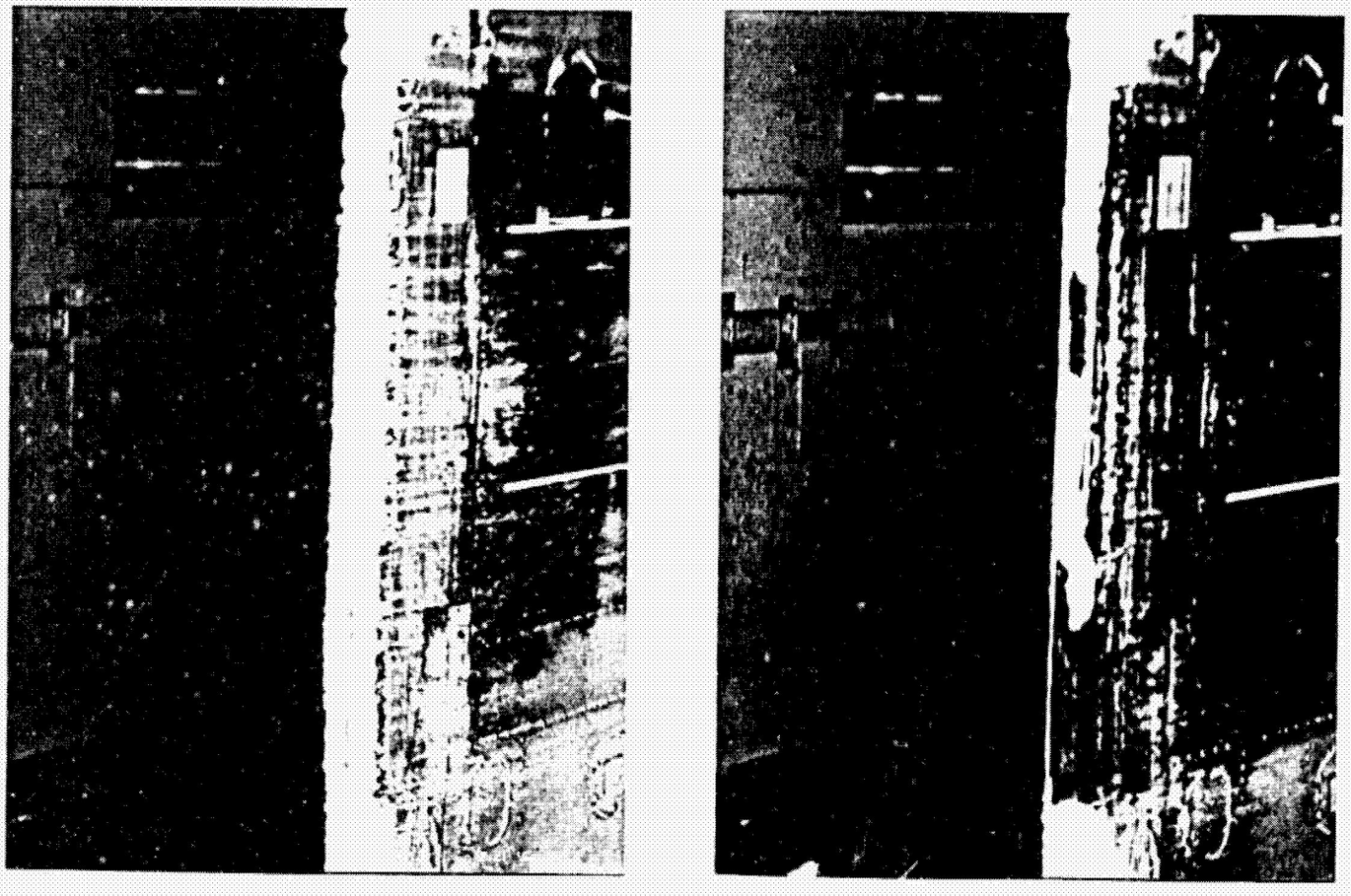

(a) Before Inflation

(b) After Inflation

Figure 21. - Run 22; α = 1.2°, V = 96 K, LWC = 2.40 gm/m^3, $\bar{d}$ = 20 μm, T = 5°F, t = 6 min.

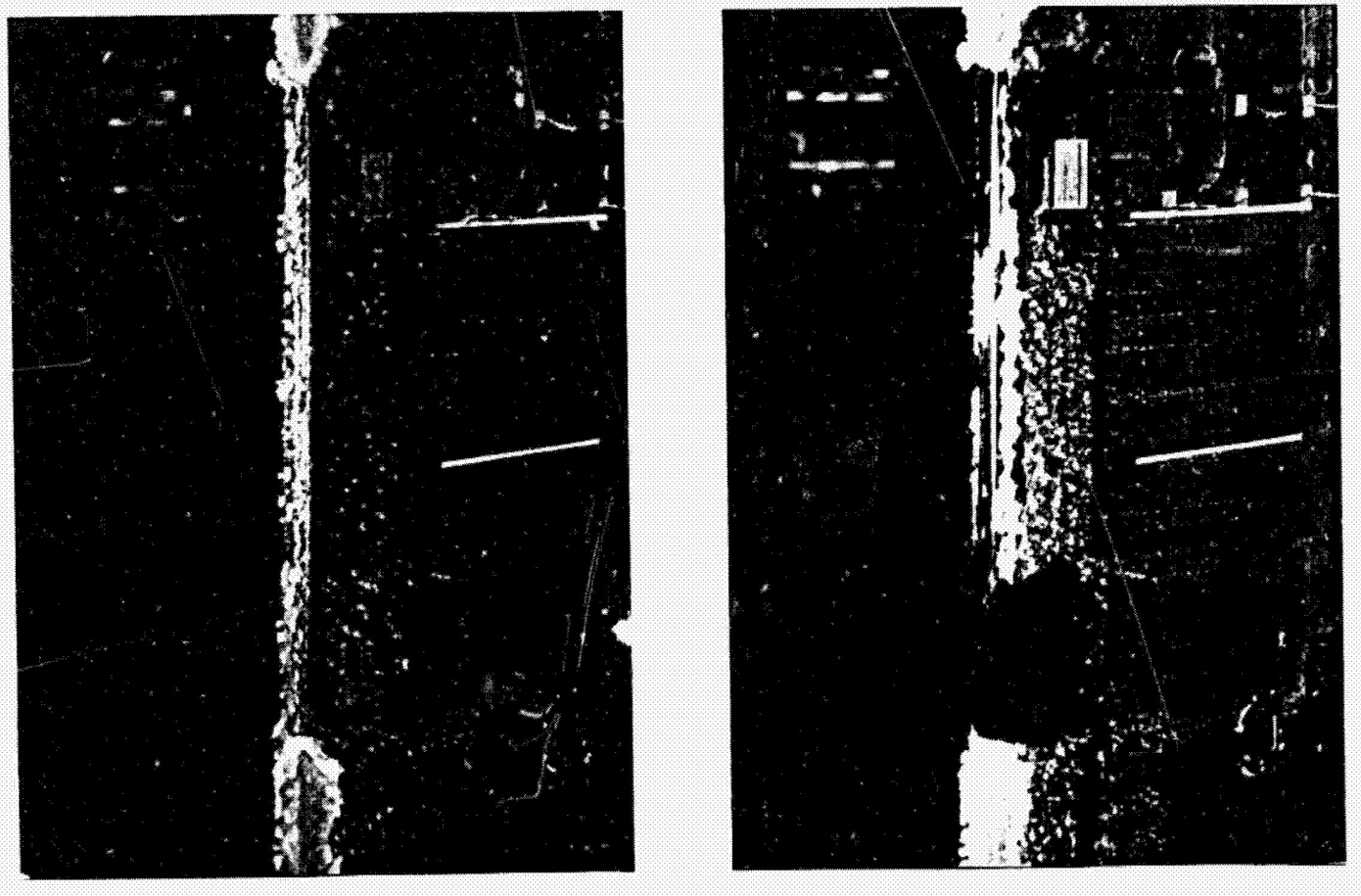

(a) Before Inflation

(b) After Inflation

Figure 22. - Run 47; α = 7.8°, V = 96 K, LWC = 2.40 gm/m^3, $\bar{d}$ = 20 μm, T = 25°F, t = 8 min.